DE GRUYTER OPEN

Acta Geophysica
vol. 63, no. 4, Aug. 2015, pp. 1150-1180
DOI: 10.1515/acgeo-2015-0020

Ionospheric and Solar Wind Variation during Magnetic Storm Onset and Main Phase at Low- and Mid-latitudes

Bolarinwa J. ADEKOYA[1] and Babatunde O. ADEBESIN[2]

[1]Department of Physics, Olabisi Onabanjo University, Ago Iwoye, Nigeria
e-mail: adekoya.bolarinwa@oouagoiwoye.edu.ng (corresponding author)

[2]Department of Physical Sciences, Landmark University, Omu-Aran, Nigeria
e-mail: f_adebesin@yahoo.co.uk

Abstract

The relationship between the F2-layer critical frequency and solar wind parameters during magnetic storm sudden commencement (SSC) and main phase periods for intense (IS) and very intense (VIS) class of storms is investigated. The analysis covers low- and mid-latitude stations. The effects of ionospheric storm during SSC period is insignificant compared to the main phase, but can trigger the latter. The main phase is characterized by severe negative storm effect at both latitudes during VIS periods while it is latitudinal symmetric for IS observations. The IS reveal positive/negative storm phase in the low-/mid-latitudes, respectively. Ionization density effect is more prominent during VIS events, and is attributed to large energetic particle and solar activity input into the earth magnetosphere. However, ionospheric effect is more significant at the low-latitude than at the mid-latitude. Lastly, ionospheric storm effect during a geomagnetic storm may be related to the combinational effect of interplanetary and geomagnetic parameters and internal ionospheric effect, not necessarily the solar wind alone.

Key words: F2 layer critical frequency, SSC, very intense storm, intense storm, driver gas, ionization density.

1. INTRODUCTION

The effects of magnetic storms on the ionosphere are complex and deviate greatly from average ionospheric behavior. The global distribution of ionospheric storm effects is also complicated and differs considerably from one storm to another. These disturbances sometimes take the form of increases/decreases of the F-layer critical frequency (*fo*F2), and are referred to as the positive/negative ionospheric storms, respectively. The propagation of negative and positive ionospheric storms is strongly determined by the thermospheric disturbance gravity waves (Liu *et al.* 2010). According to Kane (2005), positive storm effects are a result of downwelling of neutral atomic oxygen and uplifting of the F-layer due to winds. Both of these rely on large scale changes in the thermospheric circulation caused by heating in the auroral zone. The storm negative phase in *fo*F2 and total electron content (TEC) occurs in a composition disturbance zone which reaches lower latitudes in summer than in winter, and has a preference for the night and morning sectors due to the local time variation of neutral winds.

The reaction of the ionosphere as seen at different ionospheric stations may be quite different during the same storm period depending on the station coordinates, local time effects, and some other parameters (Danilov 2001, Akala *et al.* 2010, Vijaya *et al.* 2011, Adebesin *et al*. 2013). At low latitude and equatorial zone, $E \times B$ drifts are affected by prompt penetration of magnetospheric convection electric fields, as well as by long-lived dynamo electric fields from the disturbance neutral winds and storm-related changes in ionospheric conductivity (Fejer 1997). In addition, changes in the neutral composition alter the balance between production and loss in the plasma and this affects the peak density of the ionosphere. An increase in the percentage of molecular neutrals, as would be the case if the thermosphere were heated, would lead to depletion in the ionospheric density (Davis *et al.* 1997). Such effects have been reproduced by coupled models of the ionosphere-thermosphere system.

Adekoya *et al.* (2012a) had demonstrated that investigations into the origin and nature of SSC on the ionospheric F-region have continued to engage the attention of scientists who constitute the space weather community. Some of these include Prölss (1995), Mikhailov and Perrone (2009), Burešová and Laštovička (2007, 2008), and Danilov (2013). While some researchers believed that the concept of SSC is delusion, others assumed that it is a reality. Danilov (2001) listed the SSC enhancements as one of the open problems of F-region physics and suggested that perhaps soft particle precipitation in the dayside cusp or magnetospheric electric field penetration might play a role in this phenomenon. Recently, Danilov (2013) affirmed and reported the appearance of ionospheric SSC enhancement in approximately

25-30% of ordinary storms, and in almost all prominent storms. Chukwuma (2007) asserted that the difficulty with the explanation of these phenomena is because in the studies of ionospheric storms it is assumed that the beginning of the disturbance is defined by storm sudden commencement (SSC) or main phase onset (MPO), which as a scheme restricts the geoeffectiveness of the solar wind to post-onset time. These foreclose the explanation of any aspect of the morphology of ionospheric storms whose origin precedes the onset reference time. Mikhailov and Perrone (2009) assumed a criterion for selecting SSC phenomenon which is that an SSC *fo*F2 enhancement should precede the magnetic storm onset and take place within a reasonable time interval before the SSC and develop under quiet geomagnetic conditions. If an observed *fo*F2 increase does not satisfy this requirement, there is no reason to consider it an SSC enhancement. This work therefore attempts to find the relationship between ionospheric and solar wind phenomena during SSC and main phase of geomagnetic storms at some selected low- and mid-latitude stations.

2. DATA AND METHODOLOGY

The geomagnetic index and solar wind data used consist of hourly UT values of the low latitude magnetic index *Dst* [nT], the solar wind flow speed *V* [km/s], the southward interplanetary magnetic field component (IMF *Bz* component [nT]), the plasma flow pressure *P* [nPa], the proton number density [N/cm^3], the plasma temperature *K*, plasma beta, and interplanetary electric field [mV/m^2]. These data were obtained from the National Space Science Centre's NSSDC OMNIWeb Service (http://nssdc.gsfc.nasa.gov/omniweb).

In like manner, the ionospheric data used are hourly UT values of *fo*F2 obtained from Space Physics Interactive Data Resource (SPIDR's) network (http://spidr.ngdc.noaa.gov) of ionosonde stations located in the low- and mid-latitude regions. These stations are located in the Australian (Darwin, Learmonth), Euro-African (Grahamstown, Juliusruh/Rugen), and American sectors (Boulder). Their coordinates are listed in Table 1.

In order to contribute to the solution of the controversial problem of ionospheric F2 and geomagnetic storm phenomena during SSC event that leads to main phase disturbances, six intense geomagnetic storms were investigated: four very intense ($Dst \leq -250$ nT) and two intense (-100 nT $\leq Dst > -250$ nT) (*e.g.*, Gonzalez *et al.* 2002, Adebesin 2008) storms at low and low-mid latitude (Table 1). It is important to note that paucity of data at some stations during the days under investigation restricted the choice of ionosonde stations. However, the normalized deviation of the critical frequency *fo*F2 from the reference, which is used to denote the F2 region response to a geomagnetic activity, is given by

Table 1

List ionosonde stations used with their geomagnetic and geographic coordinates

Name of the ionospheric station	Station code	Geographic latitude and longitude	Geomagnetic latitude and longitude	Difference between LST and UT [hrs]
Darwin	DW41K	–12.5, 131.0	–22.90, 202.66	+9
Learmonth	LM42B	–21.9, 114.0	–34.15, 185.02	+8
Grahamstown	GR132	–33.3, 26.5	–33.92, 89.37	+2
Boulder	BC840	40.0, –105.3	48.90, 316.50	–7
Juliusruh/Rugen	JR055	54.6, 13.4	54.25, 99.73	+1

$$D(foF2) = \frac{foF2 - (foF2)_{ave}}{(foF2)_{ave}} \times 100\% \quad , \tag{1}$$

$D(foF2)$ variation is described in terms of percentage change in amplitude of the $foF2$ from the reference. According to Liu *et al.* (2008), positive and negative storms occur when the absolute maximum value of $D(foF2)$ exceeds 20%. Further, this limit is sufficiently large to prevent inclusion of random perturbation and disturbances of gravity waves, thereby making the indicated positive and negative storms represent real changes in electron density and not just redistribution of the existing plasma.

The data analyzed consist of $D(foF2)$ of respective hourly values of $foF2$ for 6-8 April 2000, 15-17 July 2000, 16-18 September 2000, 30 March – 1 April 2001, 10-12 April 2001, and 23-25 August 2005. The reference for each hour for each storm event is the average value of $foF2$ for that hour calculated from the four quiet days preceding the storm, based on the magnetic activity index ($Ap < 26$ corresponding to disturbance storm time $Dst \geq -25$) (Adeniyi 1986). Also these days are devoid of not only any significant geomagnetic activity, but also an absence of any considerable solar activity. This followed from the fact that high solar flare activity results in ionospheric disturbances due to their effects on thermospheric neutral density (Sutton *et al.* 2006).

3. RESULTS

3.1 Signature of interplanetary and geomagnetic parameters with ionospheric variations

3.1.1 Storm of 6 April 2000

Figure 1 presents the interplanetary, geomagnetic, and ionospheric observations for the 5-9 April 2000 storm event covering the initial, main, and re-

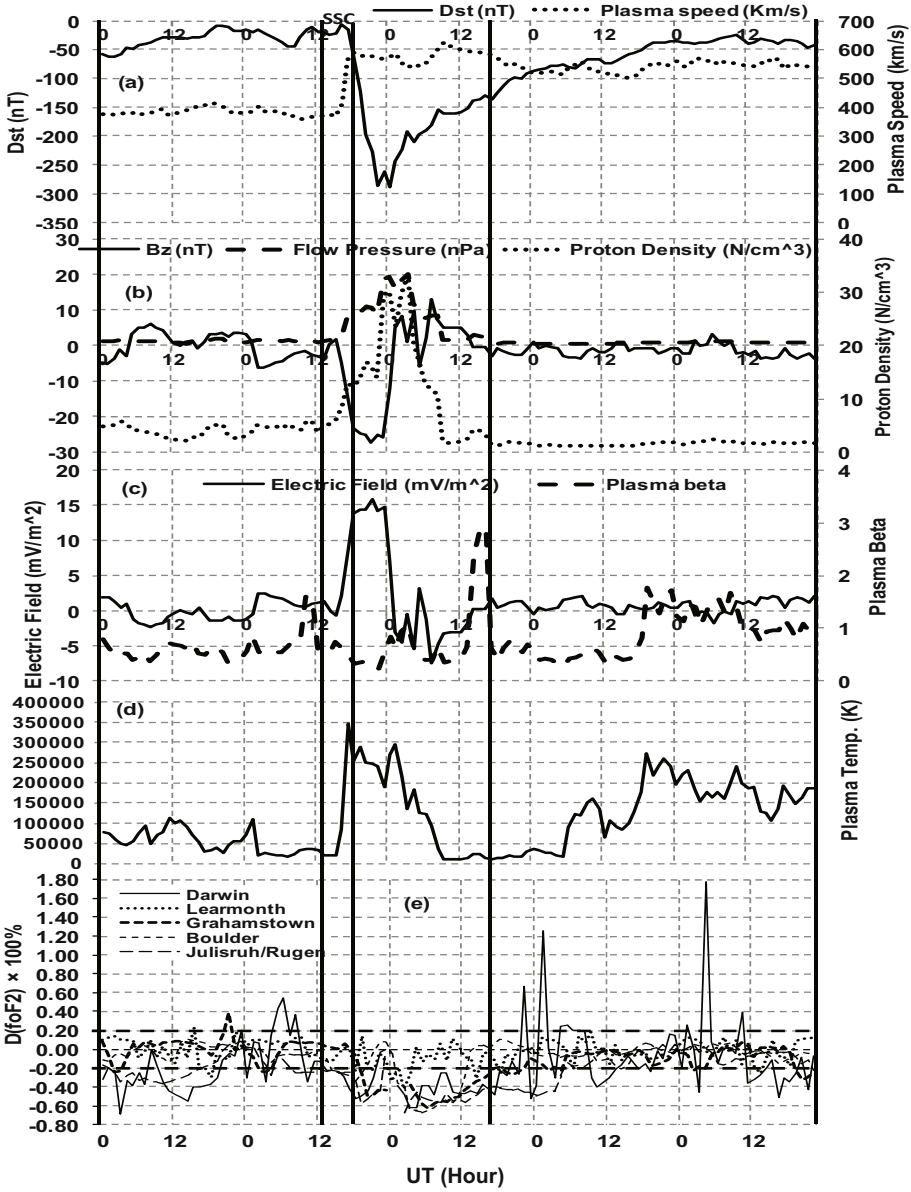

Fig. 1. Geomagnetic and interplanetary variations with *D*(*fo*F2) response during storm-time period for low- and mid-latitude stations. The storm spans 5-9 April 2000. The thick horizontal dashed lines depict the disturbed time reference level on the *D*(*fo*F2) plot.

covery phases, respectively. Figure 1a presents the geomagnetic index *Dst* (left side) and solar wind speed (right side). The storm is summarized using

available interplanetary data. However, Vieira *et al*. (2001) classified geomagnetic storm as weak (when $Dst > -50$ nT), moderate (when -100 nT < peak $Dst \leq -50$ nT), and intense (when $Dst < -100$ nT). From the early hour of 5 April the storm emerged with a moderate to weak amplitude activity up to around 12:00 UT on 6 April. Following this is the period expected to be dominated by sudden storm commencement phenomena (Balasis *et al*. 2006, Adekoya *et al*. 2012a), but the decrease in the westward ring current encircling the earth did not significantly enhanced the *H* component (little energy is entering into the earth magnetosphere). However, the *Dst* value was observed to be –6 nT around the onset period, which indicates that the storm is not preceded by SSC. The *Dst* thereafter decreases to a minimum peak value of –288 nT at 00:00 UT of the main phase. This coincided with the maximum plasma speed increase of 625 km/s at 09:00 UT. Also, this period of minimum *Dst* was observed to have an increasing plasma flow pressure with maximum peak value of 20.34 nPa at 03:00 UT (Fig. 1b). *Bz* was initially southwardly oriented with a magnitude of –27.3 nT at 21:00 UT before a northward orientation, which coincides with the *Dst* minimum peak. The proton density was initially decreased from the early hour of 5 April with decreasing average value of 3.50 N/cm^3 which lasted for about a day and a half (Fig. 1b). The high electric field experienced during the main phase coincides with the *Bz* southward turning, as well as plasma temperature. The increase in plasma pressure and electron density consequently increased the plasma temperature, as well as a lifting in the electric field drift. This temperature rise (Fig. 1d) during the main phase corresponds to increase in plasma beta of about 2.92 magnitudes (Fig. 1c). It transpires from the high plasma beta and temperature values that the onset period was followed by ejecta, which may not be magnetic cloud type. According to Dal-Lago *et al.* (2004), the interaction of the high stream and ejecta results in an increase in speed, density, and temperature.

The ionospheric F2 effect observed over the low- and mid-latitude stations are presented in Fig. 1e using a normalized deviation of the critical frequency, $D(fo\mathrm{F2})$, during the storm progression. Highlighted in the plot is the region for sudden storm commencement/storm onset (mark SSC), main phase (the region between the second and the third vertical dashed lines across the plot), and then the recovery phase. The horizontal dashed lines show the disturbed reference level. Discernible changes in the $D(fo\mathrm{F2})$ were observed at the onset, main and recovery phases of the storm, respectively, which may be the consequence of geomagnetic storm effects. Here, the maximum ionization density of the F2 layer serves as a convenient parameter to specify the ionospheric behaviour. However, ionization density may either increase or decrease during the disturbed conditions, and these changes are designated as positive and negative ionospheric storms (*P*- and *N*-storm), re-

spectively. The ionosphere at Darwin emerges with a negative ionospheric disturbance (*N*-storm) from 00:00 UT on 6 April with peak electron density variation value of 34% at 03:00 UT. Thereafter, a sharply enhancement (positive –54%) was observed around 06:00 UT before a prolonged negative storm which extended to the SSC period. The intense negative phase observation at SSC was trailed by significant negative phase storm during the main and the recovery phase was largely controlled by the intense positive storm. Similarly, Learmonth with insignificant negative ionospheric storm variation during the storm-onset period was followed by noticeable negative storm effect at post-midnight and post-noon periods with percentage magnitudes of 43 and 31% at 02:00 and 14:00 UT during the main phase. The ionospheric storm response over Grahamstown was insignificant during the marked SSC period, while the main phase was largely predominated by an intense negative phase storm as a result of the depletion in *D*(*fo*F2). The ionosphere over Boulder and Juliusruh/Rugen shows similar *D*(*fo*F2) morphology with that observed over Learmonth. The main phase at these stations was completely controlled by negative storm effect which extended into the recovery phase. It has been reported that changes in neutral composition alter the balance between production and loss in the plasma, and subsequently affects the peak density of the ionosphere. If the thermosphere were heated, the molecular neutrals percentage would increase, and would result in the depletion of the ionospheric density (Davis *et al.* 1997).

3.1.2 Storm of 15 July 2000

Depicted in Fig. 2 is the interplanetary and geomagnetic response with the corresponding ionospheric observation during a very intense storm (VIS) of 16 July 2000 (see discussion section for the storm classification). Figure 2a-d presents the interplanetary and geomagnetic observation while Fig. 2e presents the ionospheric F2 effect during the geomagnetic storm and spans 14-18 July 2000, representing the initial (storm-onset periods is embedded in the initial phase period of the storm), main and the recovery phases, respectively. The characteristic signature of this magnetic storm is the depression in magnitude of *Dst* value within 17:00 UT on 15 July to 11:00 UT of 16 July known as storm main phase (*i.e.*, the *H* component of magnetic field) (Fig. 2a). This depression was a result of the ring current encircling the Earth in the westward direction (*e.g.*, Kamide *et al.* 1998). The *Dst* value decreases greatly to a minimum value of –301 nT at 01:00 UT on 16 July. This corresponds to the increase in solar wind flow speed to a peak value of 1107 km/s. On the *Dst* plot is the picture of the sudden positive increase known as the sudden storm commencement (SSC), which is generally recently known as the SSC (see Balasis *et al.* 2006, Mikhailov and Perrone 2009, Adekoya *et al.* 2012a) and spans 12:00-17:00 UT. This period is observed to be a turning

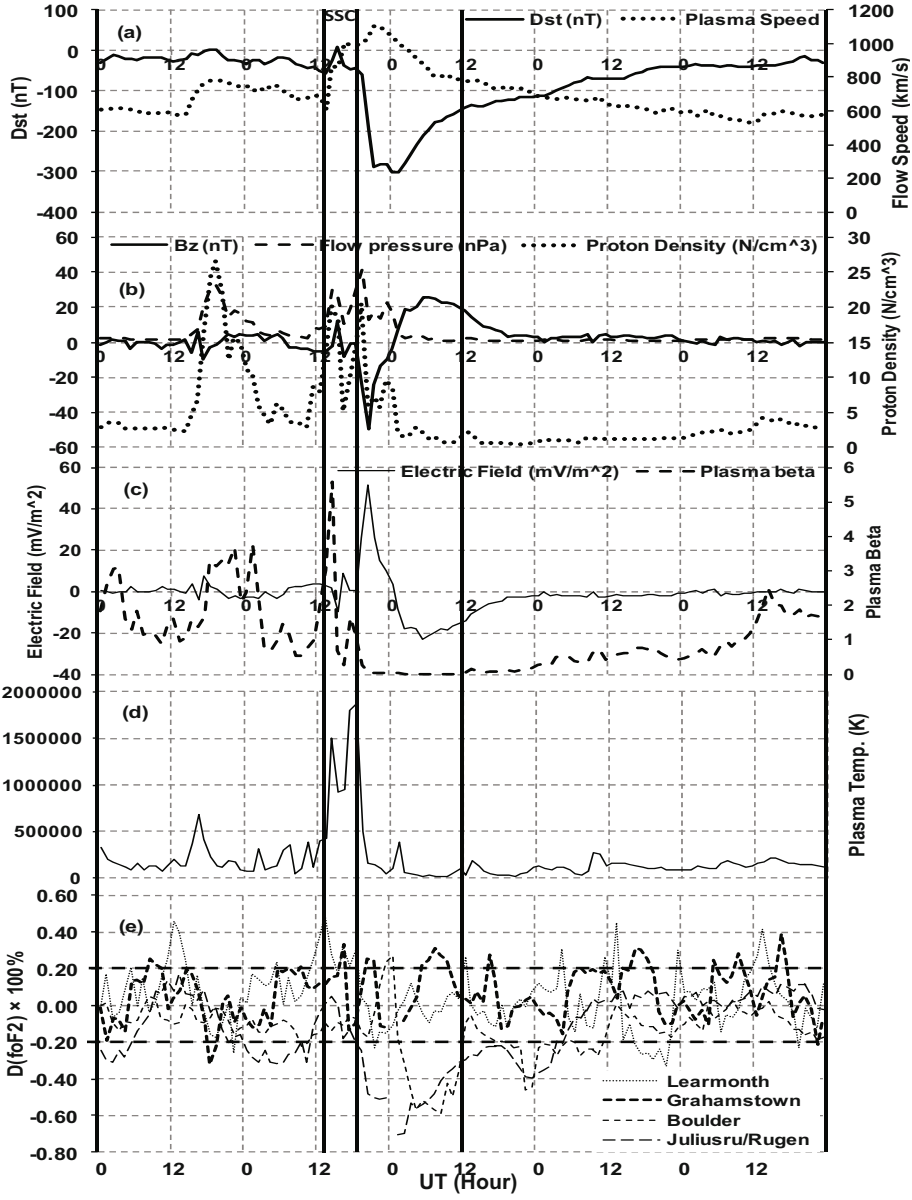

Fig. 2. Same as in Fig. 1 but for the storm of 14-18 July 2000.

point for the flow speed increase, as well as the southward orientation of IMF *Bz* (Fig. 2b). It is generally observed during this period that all the observed parameters responded with sudden changes. This is a result of the ef-

fect of compression of the front side of the magnetosphere of enhanced solar wind pressure, and subsequently increased the plasma temperature to its peak value around 17:00 UT (Fig. 2d). Consequently, the temperature decreased together with plasma beta to low values of 19 192 K and 0.03, respectively. The electric field increase to its peak value coincides with the peak southward orientation of *Bz* (–49.4 nT) and proton density (20.6 N/cm^3) at about 20:00 UT. This storm was followed by a slow recovery that lasted for over 10 hours. The storm is characterized as a magnetic cloud type, with a characteristic low plasma beta, relatively high density ratio of He^{++} to proton (Wang *et al.* 2003), low plasma temperature, and slowly varying strong magnetic field *Bz* (Gonzalez *et al.* 1999, 2002, Adekoya *et al.* 2012a).

The consequence of this storm on the ionospheric F2 layer over the low- and mid-latitude stations is presented in Fig. 2e. The horizontal dashed lines show the disturbed reference level of both positive and negative storm phases. Between the first two vertical lines is the period marked SSC. We observed that the ionospheric F2 electron density during the SSC period at Learmonth and Grahamstown was enhanced with an average *fo*F2 value of about 32%. Boulder and Juliusruh are in the Northern Hemisphere. Their *D*(*fo*F2) variation was depleted significantly compared to the Southern Hemispheric stations (Learmonth and Grahamstown) with weak positive storm appearance during the main phase. The observed ionospheric storm event during the main phase may have originated from the mass input of energetic particle that change the daytime eastward electric field at this stations. The main phase depletion could be attributed to composition changes, which directly influence the electron concentration in the F2 region. In other words, the ionospheric storm intensity is more pronounced during the main phase, and may have arise from more penetration of the connective electric field and neutral wind (*e.g.*, Foster and Rich 1998).

3.1.3 Storm of 17 September 2000

The solar wind parameters and magnetic index observation for the intense geomagnetic storm that spans 15-19 September 2000 are illustrated in Fig. 3a-d. This storm had a minimum *Dst* excursion of –201 nT. The storm-onset occurred within 12:00-21:00 UT on 17 September. The *Dst* amplitude started decreasing from around 19:00 UT and reached its minimum amplitude of –201 nT at 23:00 UT. It was accompanied with a steep drop and polarity reversal in IMF *Bz* (Fig. 3b). It turns southward and attained maximum negative value of –23.9 nT at 21:00 UT. Afterwards, there was a steep rise noticed in the northward direction. During the main phase, the solar wind speed reached a peak of 839 km/s, with a corresponding increase in flow speed during the SSC period. The compression in the earth magnetosphere subsequently increased the flow pressure and the temperature to a peak

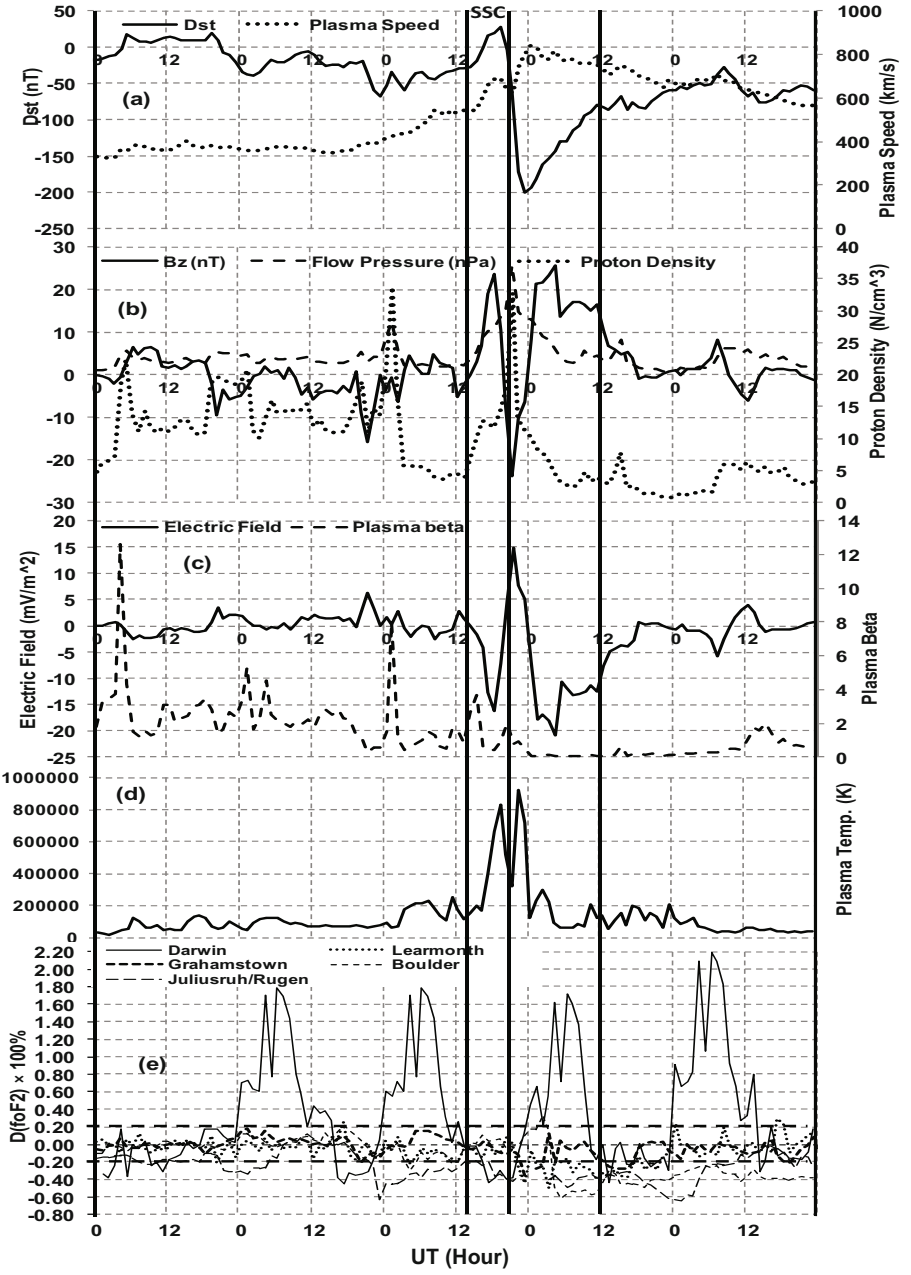

Fig. 3. Same as in Fig. 1 but for the storm of 15-19 September 2000.

value; which in effect increased the proton number density during the main phase. The electric field activity during the SSC period is observed to turn

Table 2

The distribution of storms according to their southward IMF *Bz* source

Storm date	Peak *Dst* [nT]	*V* [km/s]	*Bz* [nT]	Plasma temperature [K]	Plasma beta	Proton density [cm^{-3}]	Source of storm event
6 Apr 2000	–288	625	–27.3	L	1.06	33.4	sheath
16 Jul 2000	–301	1107	–49.4	L	0.03	9.7	cloud
17 Sep 2000	–201	839	–23.9	H	0.93	32.8	sheath
31 Mar 2001	–387	821	–44.7	H	1.61	25.2	sheath + ejecta
11 Apr 2001	–271	687	–20.5	H	1.22	24.2	sheath + cloud
24 Aug 2005	–216	721	–38.3	H	6.29	29.6	sheath + ejecta

Explanations: H – high plasma temperature (*i.e.*, $T \geq 400\,000$ K), L – low plasma temperature (*i.e.*, $T < 400\,000$ K).

southward with a reduction in magnitude up till a peak value of –16.28 mV/m^2 during the SSC period (Fig. 3c). It thereafter rotates northward and reached a peak value of 14.19 mV/m^2 during the main phase boundary. It is overwhelming that the solar wind dawn-to-dusk electric field directly drives magnetospheric convection. These electric fields are caused by a combination of increase solar wind velocity and southward IMF. This storm event was observed to be a sheath *Bz* source storm event (see Table 2 and Section 4 for more details).

The ionospheric observations to this storm are presented in Fig. 3e. The onset period occurred during the daytime of 17 September. The significant positive disturbance is majorly noticed at Darwin throughout the studied storm period, the SSC responded with depletion in electron density which was trailed by an enhanced *D*(*fo*F2) value of 168% around 05:00 UT at the main phase. The electron density variation for Learmonth, Grahamstown, Boulder, and Juliusruh/Rugen were disturbed with negative storm effect during the main phase compared to Darwin. Only Learmonth during the SSC was enhanced with noticeable storm disturbances. However, the ionospheric response over the low-latitude stations was more significant than it appears over the low latitude than in the mid-latitude of the Southern Hemisphere. Prölss (1993) had suggested that at low latitudes, the energy dissipation of the two traveling ionospheric disturbances (TIDs) launched in both hemispheres causes an increase in the upper atmosphere temperature and in the gas densities. These TIDs may be connected to the excessive and impulsive energy input in the high latitude during the storm that dissipates to the equator with high speed. The noticeable feature is that the intense main phase ionospheric storm emerged from SSC and more pronounced in the Northern Hemisphere over the mid-latitude stations.

3.1.4 Storm of 31 March 2001

Figure 4 presents the superposed plot of *Dst*, plasma flow speed, the IMF *Bz*, and other solar wind parameters together with the corresponding *D*(*fo*F2)

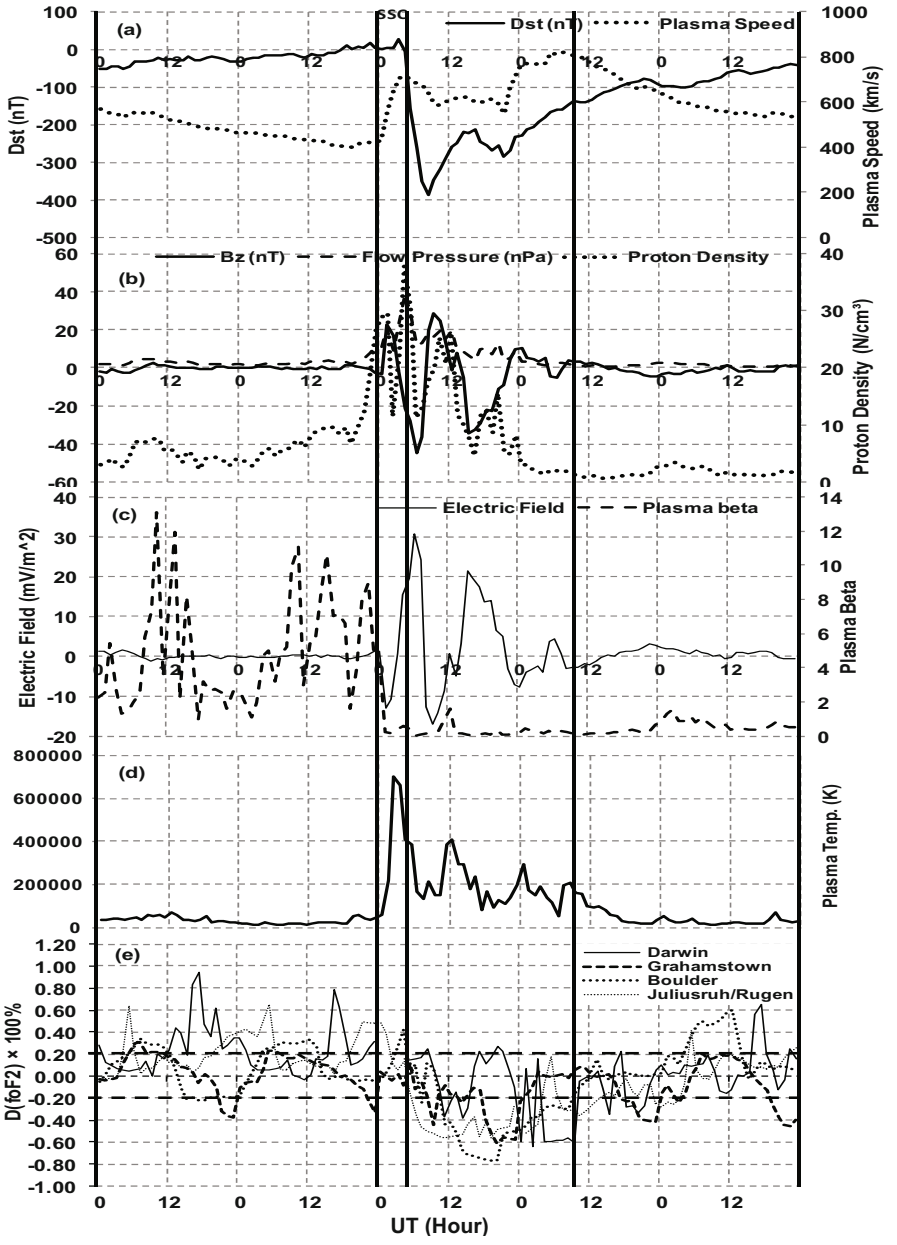

Fig. 4. Same as in Fig. 1 but for the storm of 29 March – 2 April 2001.

observations for the storm that occurred within 00:00 UT 29 March – 23:00 UT 2 April 2001. From Fig. 1a, the *Dst* plot shows a reduction in solar activity for a couple of hours at the initial phase. This progressive low storm signature continued till around 00:00 UT 31 March when a sudden positive storm enhancement was followed by a large depression in the *Dst* index to a value of –387 nT at 08:00 UT. On the contrary, the flow speed plot shows a high speed stream during the main phase of the storm with a peak value of 821 km/s. The maximum *Bz* southward orientation is observed with a peak value of –44.7 nT (Fig. 1b); this coincides with the *Dst* minimum peak value at 08:00 UT. The intense IMF is believed to be associated with essentially two activities: firstly the high-speed stream, intrinsic fields, and plasma associated with the coronal ejecta; and secondly, the shocked and compressed fields and plasma due to the collision of the high-speed stream with slower solar wind preceding it (Gonzalez *et al.* 1994). Observing Fig. 1a, b, and d, one can see that the simultaneous increase in the flow speed stream and plasma pressure may be responsible for an increase in plasma temperature during the onset period. However, the electric field was marked with an increase in northward field flow of 30.62 mV/m^2 during the main phase period. Moreover, the increase in plasma beta and high electric field orientation during the main phase may be an indicative that the storm driver gas was the ejecta associated with a southward IMF *Bz* sheath (*e.g.*, Gonzalez *et al.* 2002, Dal-Lago *et al*. 2004).

Figure 4e depicts the *D*(*fo*F2) variation for this storm. Starting from 30 March, the plot shows a concurrent increase in *D*(*fo*F2) for all the stations. This positive storm excursion was extended to the SSC period. During the SSC, the ionospheric F2 effect over Darwin and Grahamstown (in the Southern Hemisphere) was insignificant, while the effect is noticeable over Boulder and Juliusruh with a positive ionospheric storm effect. Subsequently, all the stations simultaneously depleted which resulted in an intense negative ionospheric storm at the main phase.

3.1.5 Storm observation during 11 April 2001

The plot of the response of 11 April 2001, was shown in Fig. 5. The plot spans 9-13 April 2001. Figure 5a presents the *Dst* and plasma flow speed observations. The *Dst* observation revealed moderate storm appearance at the beginning of 9 April. This dominates the first observational day. Thereafter, a progressive increase in *Dst* value > –25 nT was observed throughout the second day. Thereafter, the *Dst* decreased to –105 nT at 18:00 UT, reaching the minimum peak value of –271 nT at 23:00 UT, before a sharp recovery. The increasing plasma flow speed observed during the SSC was preceded by a low solar wind flow stream. During the period mark SSC the *Dst* was observed to be –2 nT, which is an indicative that the storm **does not preceded**

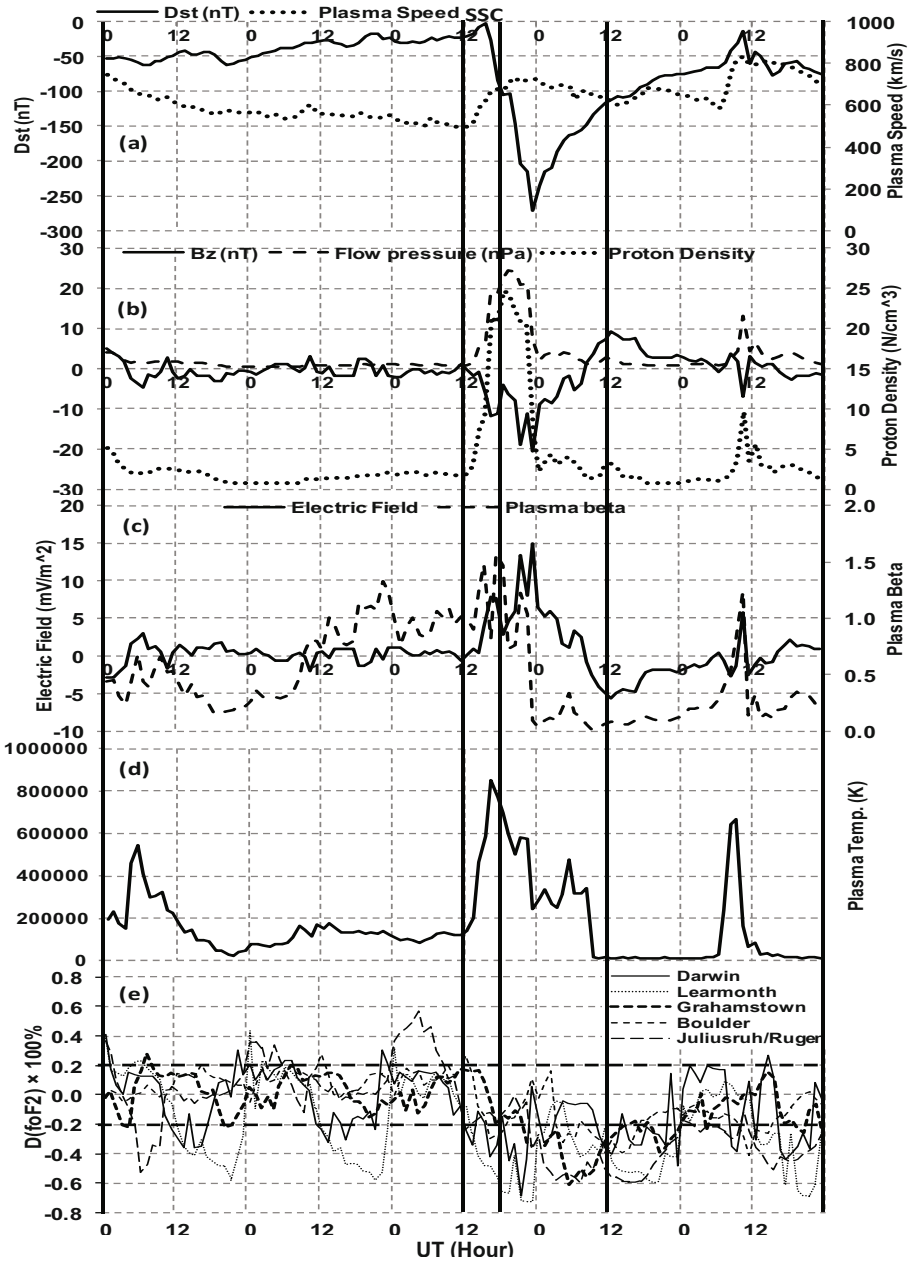

Fig. 5. Same as in Fig. 1, but for the storm of 9-13 April 2001.

by SSC. The *Bz* southward rotation emerges from the SSC period, reaching a minimum value of –20.5 nT during the main phase (Fig. 5b). As observed

in Fig. 5d, the sudden compression of the magnetosphere by solar wind increased the plasma temperature, which thereafter decreased after the impact. This as well increases the proton density and flow pressure to peak values of 24.7 N/cm^3 and 24.47 nPa at the main phase. The electric field orientation during the SSC period was northward and records a maximum field stream during the main phase. At the right hand side of Fig. 5c is the plasma beta plot. It has a relatively high value (*i.e.*, > 1) at the main phase.

Figure 5e depicts the corresponding ionospheric response. The electron density concurrently decreased during the SSC and the main phase of the storm. The ionospheric effect is more pronounced over the low-latitudes than in the mid-latitudes at both storm-onset and main phase periods. This shows an evident of latitudinal dependence. Also, the critical observation of the hemispheric dependence shows that the ionospheric storm effect is more pronounced in the Southern Hemisphere than in the Northern Hemisphere. This intense negative storm record extends to the recovery phase and decreases with time. This negative ionospheric storm effect during the main phase may be connected with a prompt eastward penetration of electric field (PPEF) and equatorward neutral winds (Balan *et al.* 2010) and change in thermospheric composition generated during geomagnetic storms at auroral latitude which are then transported to lower latitudes by the disturbed thermospheric wind circulation produced by joule heating and particle precipitation in the auroral region (Prölss 1995).

3.1.6 Storm of 22-26 August 2005

The plot of the response of this storm is as shown in Fig. 6. The plot spans 22-26 August 2005. Throughout the initial phase the storm was quiet with the *Dst* peak value not exceeding ±16 nT. During the onset period the *Dst* increases as a result of sudden positive enhancement in the *H* component to about 30 nT before it later decreases to the minimum peak value of 216 nT around 11:00 UT during the main phase. The decrease is a result of depression in the ring current encircling the Earth in the westward direction. The higher plasma density and velocity combine to form a much larger solar wind ram pressure. This pressure compresses the Earth's magnetosphere and increases the field magnitude near the equator. This *Dst* decrease is coincident with a high speed stream of solar wind with a peak of 721 km/s at 13:00 UT, high proton temperature, increased proton density, and flow pressure at 13:00 UT, as well as high southward turning of *Bz* of magnitude –38.3 nT was evident. The *Bz* later rotates northward, reaching a peak value of 19.6 nT at 13:00 UT (in Fig. 6b). However, it transpired from the concurrent enhancement in plasma beta and proton temperature that the shock produced was followed by ejecta which are not of magnetic cloud type.

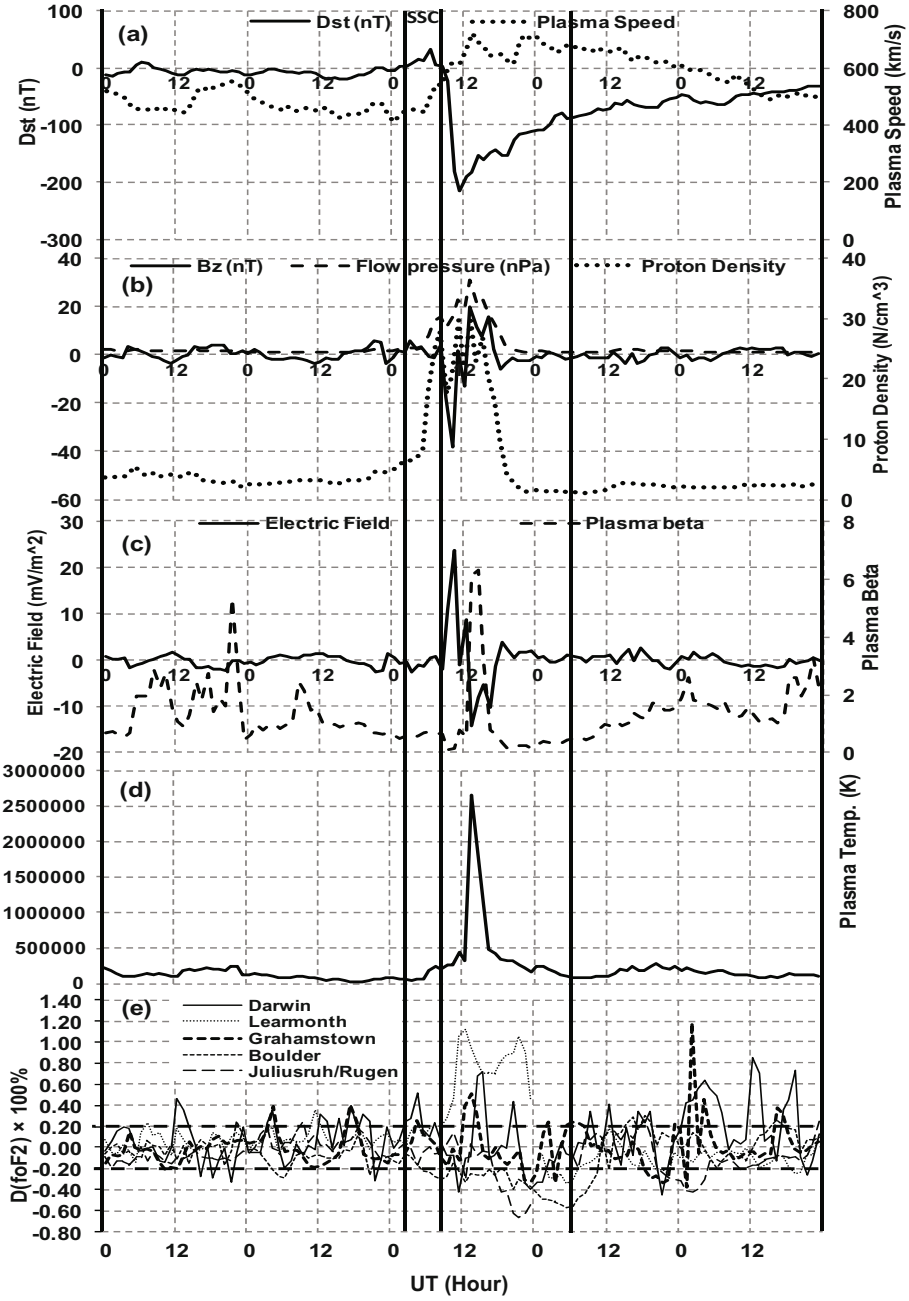

Fig. 6. Same as in Fig. 1, but for the storm of 22-26 August 2005.

Consequently, the ionospheric effect of this storm is highlighted in Fig. 6e. The plot spans 22-26 August 2005 indicating the initial, main, and recovery phases, respectively. As discussed in Section 4, the storm is an intense storm driven by complex ejecta gas. The ionospheric effect is latitudinal dependence. Severe long lasting increase/decrease of ionization at low-/mid-latitude constituted the typical ionospheric response to the intense geomagnetic storm. The $D(fo\mathrm{F2})$ wavelike variation over Darwin elongated to the SSC period with electron density increase (positive storm effect). Similarly, the ionosphere over Grahamstown had initial records of positive storm phase with a magnitude of 39% and 40% at 04:00 and 17:00 UT before the SSC period. Consequent to the storm onset, the ionosphere responded with a weak positive storm of magnitude 25%. The effect over Learmonth ionosphere is more significant during the main phase, and insignificant during both initial and recovery phases. The ionosphere over Boulder and Juliusruh/Rugen shows similar $D(fo\mathrm{F2})$ pattern during the main phase. Their respective SSC period response appears to be negative with weak amplitude at Boulder, and Juliusruh experiencing quiet condition. The main phase over both stations was abruptly depleted with a significant negative storm impact.

4. DISCUSSION AND COMPARISON WITH PREVIOUS RESULTS

According to Gonzalez *et al*. (2002), the dominant interplanetary phenomena that are frequently associated with intense magnetic storms are the interplanetary manifestations of fast coronal mass ejections (CMEs). Two such interplanetary structures, involving an intense and long duration *Bs* component of the IMF are: the sheath region behind a fast forward interplanetary shock, and the CME ejecta itself. These structures, when combined, lead sometimes to the development of very intense storms, especially when an additional interplanetary shock is found in the sheath plasma of the primary structure accompanying another stream (Gonzalez *et al*. 2002). For the intense magnetic storms (IS) ($-250\ \mathrm{nT} \le Dst < -100\ \mathrm{nT}$) and very intense magnetic storm (VIS) ($Dst \le -250$ nT), the solar wind speed and the IMF intensity must be substantially higher than their "average" values of $V \approx$ 400 km/s, $Bz = -10$ nT and over a period exceeding 3 h (Gonzalez and Tsurutani 1987, Gonzalez *et al*. 2002, Vieira *et al*. 2001, Adebesin 2008, Adebesin and Chukwuma 2008). With the aforementioned geomagnetic storm classification and characteristics, it is obvious that the storms of 7-9 April 2000, 16-18 July 2000, 29 March – 2 April 2001, and 9-13 April 2001 are very intense storms (VIS), while the storms of 17-19 September 2000 and 22-26 August 2005 are intense geomagnetic storm (IS). Moreover, some geomagnetic storms, especially the largest one, begin with a sudden impulse which signals the arrival of an interplanetary shock structure (Gonzalez *et al*.

2002). This generally coincides with the onset of a period of increased ram pressure (initial phase).

We highlighted in Table 2 the distribution of storms according to their IMF *Bz* sources. According to Gonzalez *et al*. (2007), there are several drivers that are responsible for the excitation of disturbed conditions. These are: (i) the corotating interactive region (CIR), which in many cases may be associated with high speed stream; (ii) the interplanetary coronal mass ejections (ICME) which are the main causes of magnetic cloud (MC) driver; (iii) the "Sh + MC" for a sheath *Bs* (*Bz* southward) field which is followed by a magnetic cloud; (iv) the "S compressed MC" for a magnetic cloud compressed by a shock; and (v) "Complex" for a case in which none of the other cases were identified. However, Echer *et al*. (2005) classified the magnetic cloud as having high magnetic field strength, smooth rotation in the *Bz* or *By* component, low proton temperature, and plasma beta. The sources of the interplanetary southward magnetic field, *Bs*, responsible for the occurrence of the storms were related to the intensified shock/sheath field, interplanetary magnetic cloud's field, or the combination of sheath-cloud or sheath-ejecta field (Dal Lago *et al*. 2004). Only the storm of 16 July 2000 is observed to be driven by MC, while all others are either driven by sheath and cloud, sheath followed by ejecta, or ordinary sheath (see Table 2). Echer *et al*. (2005 and reference therein) have reported the occurrence of low proton temperature in solar wind at main phase and postulated the existence of magnetic cloud. Furthermore, they characterized the driver gas region by low solar wind proton density and temperature associated with intense and smooth magnetic fields during a visualization of the evolution of the ICMEs in interplanetary space. Sometime within the gas, strong north-south IMF orientations occur. This occurs mainly in a low plasma beta within an interval of 0.03-0.8, with 0.1 typical (*e.g.*, Choe *et al*. 1992). We found here for the MC driver gas, a low plasma beta of 0.03, low proton density of 9.7, high north-south IMF component, and low plasma temperature, which are common ICME driver characteristics.

During a geomagnetic storm, the disturbed solar wind-magnetosphere interactions could affect the low- and mid-latitude ionospheric F region due to intense transient magnetospheric (prompt or direct penetration) convective electric fields and neutral air wind (ionospheric disturbance dynamo) (Adekoya *et al*. 2013 and references therein), which result in changes to rates of production and loss of ionization. These electric fields redistribute the plasma, affecting production and loss rates (Buosanto 1999). Storm-related electric fields may also destabilize the plasma, producing irregularities. It is to be noted that ionization density may either increase or decrease during disturbed conditions, and these changes are traditionally designated as positive and negative ionospheric storms, respectively. A decrease in the

mean molecular mass (increasing the O density relative to N_2 and O_2) from downwelling through constant pressure surfaces would lead to increases in electron density (positive storm) while an increase in the mean molecular mass (*i.e.*, decreases in the O/N_2 and O/O_2 neutral density ratios) due to upwelling leads to decreases in electron density (negative storm) (Buosanto 1999). Mikhailov *et al*. (1995) reported that an increase in the O density is more important than an increase in the O/N_2 ratio in causing positive storm effects. Parameters such as latitude, hemispheric, and phase of the storm are crucial for determining the occurrence and magnitude of the positive and negative storm effects. Many observations and modeling studies have shown the mechanisms that are responsible for these storm time effects.

Though many attempts are going on, there remain gaps in the present understanding of how the ionosphere responds to geomagnetic storms. Danilov (2001) had explained the principal features of the positive and negative phase distribution and variations on the basis of the principal concept: during a geomagnetic disturbance there is an input of energy into the polar ionosphere, which changes thermospheric parameters, such as composition, temperature, and circulation. Composition changes directly influence the electron concentration in the ionospheric F2 region. The circulation spreads the heated gas to lower latitudes. The conflict between the storm-induced circulation and the regular one determines the spatial distribution of the negative and positive phases in various seasons. According to Davis *et al.* (1997), large ionospheric currents cause joule heating of the atmosphere and if these currents are sufficiently long lived, they can cause an upwelling of the neutral thermosphere, bringing more molecular species such as N_2 and O_2 to the height of *fo*F2. At F region altitudes, these molecules are converted into molecular ions by charge exchange or ion-atom interchange reactions with oxygen ions and then relatively rapidly undergo dissociative recombination to cause depletion in the F region plasma density. The origin of negative ionospheric storms is well understood. It is attributed to changes in the composition of neutral density in response to a storm, which will take place only after sufficient particle precipitation from the auroral oval.

Danilov (2013) has recently proposed in his comprehensive review paper that SSC enhancements could occur in the absolutely geomagnetically quiet background, so it could not be related directly to geomagnetic activity but manifests some sort of interaction between the ionosphere and neutral atmosphere (the coupling from below) to geomagnetic activity. However, around this period, littlie energy is entering into the earth magnetosphere, which significantly decreases the ring current encircling the earth magnetosphere in westward direction (*e.g.*, Gonzalez *et al*. 1994, Kamide *et al*. 1998). The storms of 6 April 2000 and 11April 2001, are not preceded by SSC, so there storm onset may not be associated with SSC. The observed

D(*fo*F2) variation for the five ionospheric stations in the low and low-mid latitude did not show a concomitant variation during sudden storm commencement, main phase and the recovery phase, respectively. At low latitude the SSC period is recorded with a weak storm appearance and mid latitude stations remains in quiet mode. This may result from the fact Adekoya *et al*. (2012a) raised. They reported that ionospheric F2 response during the SSC period is thought puzzling; they may either increase or decrease or remain in quiet mode. Also, they reported that low to moderate variation in the ionospheric F2 during SSC may signal the upcoming of large ionospheric disturbances at the main phase.

Liu *et al*. (2008) studied the enhancement of the electron concentration in the ionosphere during three geomagnetic storms (21 April 2001, 29 May 2003, and 22 September 2001) using ionosonde observations and total electron content measurement along the 120°E meridian in the Asia/Aus- tralia sector. All three events show quite similar features. The strong SSC enhancements during these events are simultaneously presented in *fo*F2 and TEC and enhancements have latitudinal dependence, tending to occur at low latitudes with maxima near the northern and southern equatorial ionization anomaly (EIA) crests and depletions in the equatorial region. This is quite different from what was reported by Burešová and Laštovička (2007) for middle latitudes. They found no systemic latitudinal dependence in SSC enhancements over European region. However, the difference in the latitudinal and longitudinal intervals considered in both papers could be a natural explanation of that difference (Danilov 2013). An SSC is a period during which little energy is entering into the earth magnetosphere regardless of the speed and number of density of particle in the solar wind. This is referred to as the "pre-storm" period in other related literatures (*e.g.*, Kane 1975, Burešová and Laštovička 2007, 2008, Mikhailov and Perrone 2009, Adekoya *et al*. 2012a, Danilov 2013).

Prior to the storms, some of the stations recorded some degree of positive/negative ionospheric effect. This was consistent with earlier studies of Kane (1975). He pointed out that sometimes there appears positive phase of an ionospheric storm before the SSC of a magnetic storm. Blagoveshchensky and Kalishin (2009) carried out a detailed study of positive phases of ionospheric storms preceding SSC. They came to a conclusion that ordinary mechanisms operating during the main phases of the magnetic storm cannot provide the necessary enhancement in *fo*F2 prior to the storm. The sudden decrease in the intensity of electron density during the SSC period was immediately followed by a severe response during the main phase.

Furthermore, it is very important to note the discernible changes between the latitudinal ionospheric effect during IS and VIS events. During the IS, the atmosphere at the low-latitude region responded with an intense positive

ionospheric storm effect and the effect was *vice versa* over the mid-latitude station. This observation was consistent with the recent work of Adekoya and Adebesin (2014) and Adebiyi *et al*. (2014). However, the ionospheric effect is higher in the low latitude than it appears in the mid-latitude. The *D*(*fo*F2) variation is concurrent during VIS, the ionosphere is dominated by intense negative storm. This simultaneous depletion in the *D*(*fo*F2) at the main phase during the VIS event may be connected with a substantial increase in the average values of the solar wind parameters and the interplanetary magnetic field. Observing the latitudinal dependence at the low and mid-latitudes during the main and the recovery phases of the storm, the negative ionospheric storm effect at the main phase was followed by a positive storm during the recovery phase at low-latitudes and overturned at the mid-latitudes. The mid-latitude was generally depleted with a negative storm effect prior to variation during the SSC period. This is consistent with the results obtained by Adebiyi *et al*. (2014) and Adekoya *et al*. (2012b). Adekoya *et al*. (2012b) had investigated the effect of geomagnetic storm on middle latitude ionospheric F2 during the storm of 2-6 April 2004, and reported that positive-negative (PN) storm phase in *D*(*fo*F2) variation during SSC will signal the upcoming of an intense negative storm during the main phase. For the observed low latitudes, the low, negative storm (N) variation during the SSC is trailed by a severe negative storm effect of the main phase. If ionospheric storms show an initial positive excursion followed by negative, it is classified as PN-storms (*e.g.*, Vijaya *et al*. 2011). Furthermore, regardless of the peak variation of *fo*F2 at the initial phase, the pre-storm period is always characterized with low ionospheric storm which is immediately followed by an intense ionospheric variation at the main phase.

Tables 3 and 4 presents the peak deviation of the ionospheric critical frequency *D*(*fo*F2) during the SSC and main phase period for each of the geomagnetic storm events at the low and mid-latitude stations with their corresponding peak values of *Dst* index, solar wind parameters (*i.e.*, flow speed (*V*), southward interplanetary magnetic field (IMF *Bz*), and plasma pressure (*P*)) as well as the combine solar wind speed, and the *Bz* (*VBz* field) at the main phase; they all follow into the sun-Earth's magnetosphere-ionosphere coupling. Figures 7a and b show the regression plots for the ionospheric F2 variation with the aforementioned geomagnetic storm parameters for each of the five ionospheric stations during the main phase period; this is clarified in Table 5. Both tables, however, present the correlation coefficient between *D*(*fo*F2) and the corresponding peak values of *Dst*, solar wind parameters and *VBz* field, respectively. However, it is imperative to note that not all the observed storms are preceded by SSC. However, those that are preceded by SSC are associated with high solar wind speed (*i.e.*, $V \geq$ 700 km/s). SSC or storm onset periods resulted from the sudden decrease in

Table 3

The peak values of geomagnetic, solar wind phenomena, and ionospheric stations *D*(*fo*F2) peak variation at main phase

Storm date	Peak value of solar wind phenomena at main phase					Ionospheric stations *D*(*fo*F2) peak variations at main phase				
	Peak *Dst* [nT]	*V* [km/s]	*Bz* [nT]	Pressure [nPa]	*VBz* [nT]	Darwin	Learmonth	Grahamstown	Boulder	Juliusruh/Rugen
6 Apr 2000	–288	625	–27.3	20.34	17062.5	–0.63	–0.43	–0.59	–0.67	–0.67
16 Jul 2000	–301	1107	–49.4	41.20	57798.0	–*	–0.23	0.31	–0.59	–0.71
17 Sep 2000	–201	839	–23.9	25.54	20052.1	1.68	–0.49	–0.34	–0.63	–0.49
31 Mar 2001	–387	821	–44.7	20.78	36698.7	–0.64	–	–0.61	–0.77	–0.56
11 Apr 2001	–271	687	–20.5	24.47	14083.5	–0.68	–0.72	–0.61	–0.31	–0.60
24 Aug 2005	–216	721	–38.3	30.98	27614.3	0.72	1.12	0.50	–0.57	–0.67

*)no data available

Table 4

The peak values of geomagnetic, solar wind phenomena, and ionospheric stations *D*(*fo*F2) peak variation for storm-onset period

Storm date	Peak value of solar wind phenomena during SSC					Ionospheric stations *D*(*fo*F2) peak variations during SSC				
	Peak *Dst* [nT]	*V* [km/s]	*Bz* [nT]	Pressure [nPa]	*VBz* [nT]	Darwin	Learmonth	Grahamstown	Boulder	Juliusruh/Rugen
6 Apr 2000	–6	564	1.8	8.13	1015.2	–0.52	–0.23	0.06	–0.33	–0.28
16 Jul 2000	28	610	11.6	30.15	7076.0	–*	0.32	0.33	–0.06	0.05
17 Sep 2000	7	687	23.7	8.34	16281.9	–0.39	–0.10	–0.07	0.11	–0.41
31 Mar 2001	26	703	22.9	38.7	16098.7	0.16	–	–0.08	0.43	0.49
11 Apr 2001	–2	670	1.31	19.3	877.7	–0.42	–0.55	0.16	0.27	–0.17
24 Aug 2005	32	545	5.9	14.24	3215.5	0.52	0.23	0.25	–0.28	–0.16

*)no data available

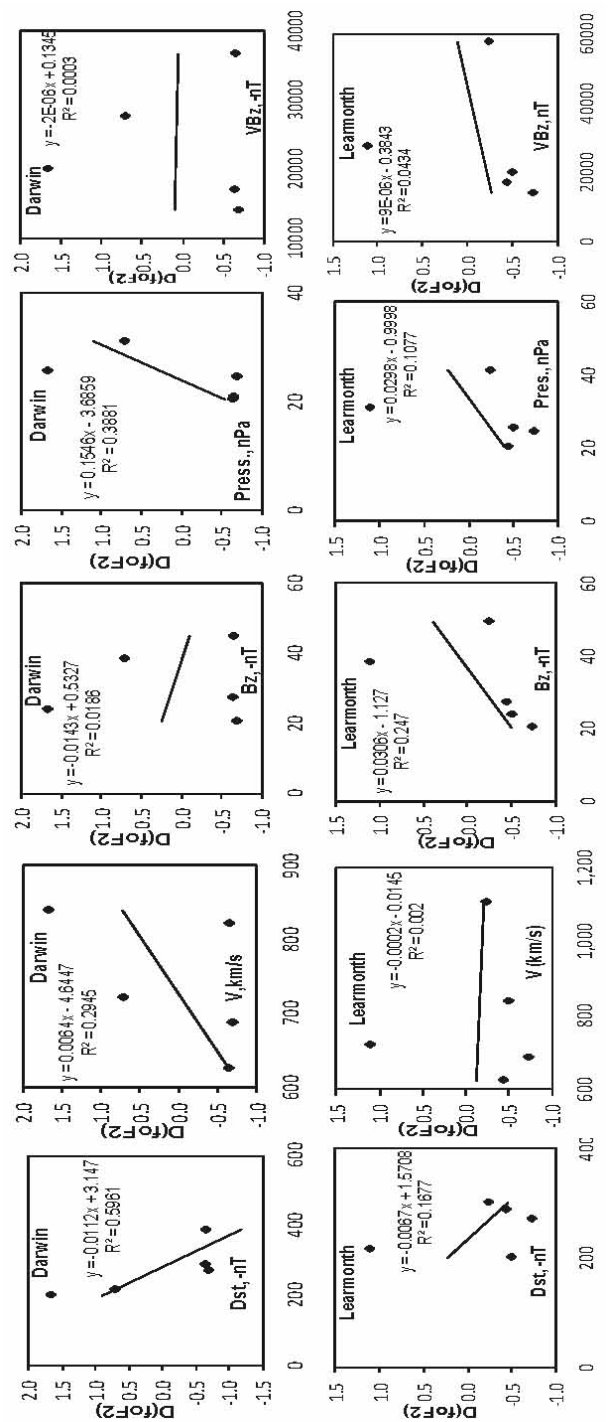

Fig. 7a. Showing the regression plots for ionospheric $D(foF2)$ peak variations with *Dst* (first column), plasma flow speed *V* (second column), IMF *Bz* (third column), plasma pressure (fourth column), and *VBz* (last column) for low-latitude stations for the years under consideration at the main phase.

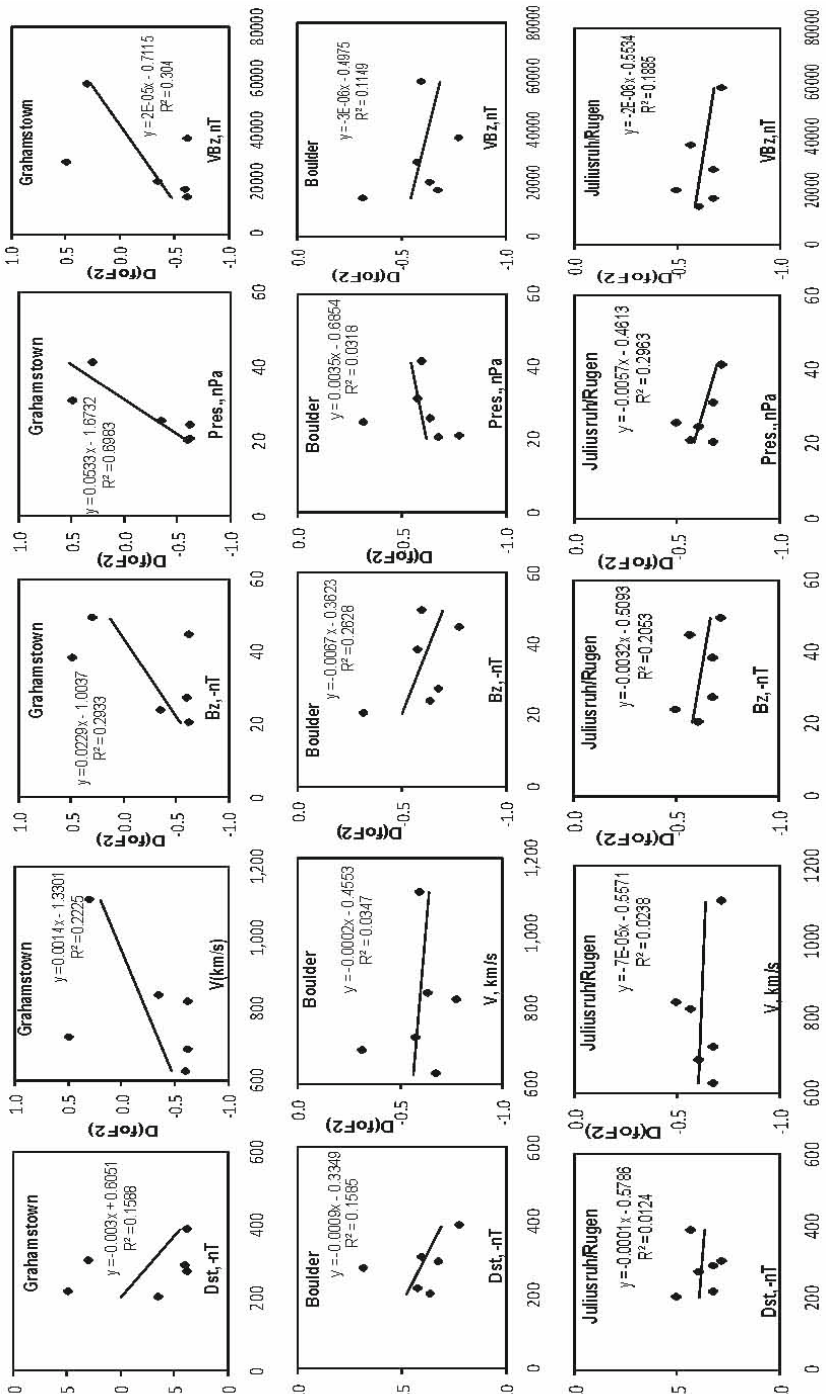

Fig. 7b. Same as in Fig. 7a, but for mid-latitude stations.

Table 5

Correlation coefficient of *D*(*fo*F2) variations during each of the 6 storm events *versus Dst*, *V*, *Bz,* plasma pressure, and *VBz* at main phase respectively; for each of the 5 stations

Stations	Latitude position	*D*(*fo*F2) *vs* peak *Dst* [nT]	*D*(*fo*F2) *vs V* [km/s]	*D*(*fo*F2) *vs Bz* [nT]	*D*(*fo*F2) *vs P* [nPa]	*VBz* [nT]
Darwin	Low	0.772	0.543	0.136	0.623	0.017
Learmonth	Low	0.410	0.045	0.497	0.328	0.208
Low latitude average		0.591	0.294	0.317	0.476	0.113
Grahamstown	Mid	0.399	0.472	0.542	0.836	0.551
Boulder	Mid	0.398	0.186	0.513	0.178	0.339
Juliuruh/Rugen	Mid	0.111	0.154	0.453	0.544	0.434
Mid latitude average		0.303	0.271	0.502	0.519	0.442
Total averaged		0.418	0.280	0.428	0.502	0.310
Aprox. total averaged [%]		42	28	43	50	31

Note: The total averaged is the mean correlation coefficient for each variable plotted against *D*(*fo*F2).

the ring current encircling the earth's magnetosphere and subsequently suddenly enhanced the *H* component (*i.e.*, *Dst*) of the field. This generally coincides with the onset of a period of increased ram pressure (initial phase) that is followed by sustained southward IMFs (main phase) and then by a return-to-normal condition (the recovery phase) (*e.g.*, Gonzalez *et al*. 1994). Consequently, the large class of storms is characterized with flow speed exceeding 700 km/s and begins with SSC.

Figures 7a and b present the regression scatter plots for the ionospheric F2 stations under investigation during the main phase of the aforementioned geomagnetic storms. The first column presents the regression plots of *Dst* [nT], the second for *V* [km/s], third for *Bz* [nT], fourth for *P* [nPa], and fifth for *VBz* [nT] in that order against their corresponding ionospheric F2 response for the low- and mid-latitude stations under consideration. The summary of the correlation values are highlighted in Table 5. It was observed that the correlation of *D*(*fo*F2) against *Dst* is more appreciative for Darwin, with percentage coefficient of 77% when compared to other stations. The corresponding ionospheric F2 variation against flow speed *V* [km/s] is depicted in the second column in Fig. 7a. It can be seen from the scatter plot and Table 5 that only Darwin showed a better correlation between *D*(*fo*F2)

and *V*. The correlation coefficient is 54% compare to Grahamstown (47%), Boulder (18%), Juliusruh/Rugen (15%), and Learmonth (4%). In relation to *Bz*, it was observed that Grahamstown (54%) and Boulder (51%) have a good correlation, its relationship with Learmonth was approximately (50%) better compared to Juliusruh (40%) and Darwin (13%). However, only Learmonth and Boulder show an almost insignificant correlation between *D*(*fo*F2) and plasma pressure. The average sum of the low- and mid-latitude values are use in observing the latitudinal dependence. At low-latitudes, only *Dst* is the main feature for ionospheric storm, with average percentage correlation of 59%. However, at mid-latitude, *Bz* and plasma pressure are the deterministic feature for causing intense ionospheric storm. Adebesin and Kayode (2012) have suggested that at high- and mid-latitude flow speed is the most geoeffective parameter with the F2 ionosphere. However, the present studies confirmed that at low-latitude *Dst* is the most geoeffective, while plasma pressure (52%) and *Bz* (54%) might be the important parameters causes ionospheric F2 variation at mid-latitude.

Moreover, it should be noted that the ionospheric F2 effect over the low-latitude region is more significant than it appears over the mid-latitude stations during the VIS events. The effect overturned during the IS event. This may be associated with the internal ionospheric effect and not necessary solar wind criteria feature alone. This is because the correlation between *D*(*fo*F2) and solar wind parameters did not show much significance in their coefficients except for the *D*(*fo*F2) and *Dst*. Although, the persistency of solar wind critical feature in the magnetosphere is as a result of combinational solar wind and internal magnetospheric activity rather than solar wind variation alone (Balasis *et al*. 2006). As a consequence, we combined the solar wind plasma speed (*V*) and the southward interplanetary field (*Bz*) to look at their relationship with the *D*(*fo*F2), since the *VBz* is the most geoeffective solar wind variables with *Dst* index (Balasis *et al*. 2006, Bakare and Chukwuma 2010). Their relationship shows on the average a poor correlation (see Table 5), the low-latitude average is 11%, mid-latitude average is 44%, and the overall average is 31%. The consequent of this is that the increase in the ionospheric effect during geomagnetic storm may be related to the combination of interplanetary and geomagnetic parameters, and internal ionospheric effect rather than solar wind variation alone.

5. SUMMARY AND CONCLUSION

We have presented the relationship between ionospheric F2 and solar wind phenomena during the SSC and main phase of geomagnetic storms for six (6) geomagnetic storms. Two are intense ($-100\ \text{nT} \leq Dst > -250\ \text{nT}$) and four are very intense ($Dst \leq -250\ \text{nT}$) in the low and low-mid latitudes. The SSC phenomena that lead to an intense ionospheric positive and negative

storm phase during the *Dst* minimum were investigated. These are *Dst* positive increase, southward turning of *Bz* (≤ -10 nT), increase in plasma speed, and high plasma pressure for both low- and low-mid-latitudes. It is pertinent to note that the largest geomagnetic storm with flow speed exceeding 700 km/s begins with SSC. Saranya *et al*. (2011) found that *Dst* index has no influence on the pre-storm enhancement phenomenon. Blagoveshchensky and Kalishin (2009) assumed that the mechanisms of the pre-storm enhancements are related to the impact of rapid particles in the foreshock region of the solar wind on the Earth's magnetosphere. Regardless of the peak variation of *D*(*fo*F2) the SSC period is always characterized with low ionospheric storm, which is immediately followed by an intense ionospheric variation during the main phase. The implication is that ionospheric storm during SSC period is insignificant compared to the main phase but can trigger the main phase storm phenomenon. Only one out of the entire storms is driven by magnetic cloud gas, which is the common ICME driver.

We observed that ionospheric storm effect during SSC is latitudinal symmetric. It is more pronounced at the low-latitude with negative storm effect than at mid-latitude with positive storm effect. However, the main phase is characterized with severe negative storm effect at both latitudes during VIS event periods. This is attributed to the large energetic particle and solar activity input into the earth magnetosphere. The negative ionospheric storm effect at the main phase was followed by a positive storm during the recovery phase at low-latitudes and overturned at mid-latitudes. In contrary during the IS, the atmosphere at the low-latitude region responded with an intense positive ionospheric storm effect and the effect was *vice versa* over the mid-latitude station. In a nut shell, the ionospheric effect is more significant in the low-latitude than at mid-latitude.

Additionally, SSC period is the quality of upcoming geomagnetic storm and ionospheric disturbance. Adekoya *et al*. (2012a, b) had suggested that SSC period might be related to some kind of pathway for penetration of energy into the terrestrial ionosphere and magnetosphere at the main phase. The recovery phase is simultaneously depleted with a significant ionospheric storm effect throughout the studied geomagnetic storm events across the latitude except for Darwin whose ionosphere responded with a severe positive storm during 6-8 April 2000 event.

The poor correlation between the solar wind parameters and *D*(*fo*F2) indicates that increase in ionospheric storm effect during geomagnetic storms may be related to the combination effect of interplanetary and geomagnetic parameters and internal ionospheric effect. At low-latitude *Dst* is the most geoeffective, while plasma pressure (52%) and *Bz* (54%) might be the important parameters causing ionospheric F2 effect at mid-latitudes. The ionospheric F2 effect over the low-latitude region is more significant than it

appears over the mid-latitude stations during the VIS while the effect is overturned during the IS period.

Acknowledgement. The authors are grateful to working team of National Space Science data Centres (NSSDC's) OMNI database (http://nssdc.gsfc.nasa.gov/omniweb), and also to the National Geophysical Data Center's SPIDR (Space Physics Interactive Data Resource) network's (http://spidr.ngdc.noaa.gov). The authors also appreciate the reviewers for the constructive comments on the structure of the paper and for their useful suggestion. This has tremendously improved the quality of the paper.

References

Adebesin, B.O. (2008), Roles of interplanetary and geomagnetic parameters in "intense" and "very intense" magnetic storms generation and their geoeffectiveness, *Acta Geod. Geoph. Hung*. **43**, 4, 383-408, DOI: 10.1556/AGeod. 43.2008.4.2.

Adebesin, B.O., and V.U. Chukwuma (2008), On the variation between D_{st} and IMF B_z during "intense" and "very intense" geomagnetic storms, *Acta Geod. Geoph. Hung.* **43**, 1, 1-15, DOI: 10.1556/AGeod.43.2008.1.1.

Adebesin, B.O., and J.S. Kayode (2012), On the coexistence of ionospheric positive and negative storm phases during January–December, 2000 geomagnetic activities at East Asian Sector, *Adv. Appl. Sci. Res.* **3**, 1, 349-370.

Adebesin, B.O., S.O. Ikubanni, S.J. Adebiyi, and B.W. Joshua (2013), Multi-station observation of ionospheric disturbance of March 9, 2012 and comparison with IRI-model, *Adv. Space Res.* **52**, 4, 604-613, DOI: 10.1016/j.asr.2013.05.002.

Adebiyi, S.J., I.A. Adimula, O.A. Oladipo, B.W. Joshua, B.O. Adebesin, and S.O. Ikubanni (2014), Ionospheric response to magnetic activity at low and mid-latitude stations, *Acta Geophys*. **62**, 4, 973-989, DOI: 10.2478/s11600-014-0205-x.

Adekoya, B.J., and B.O. Adebesin (2014), Hemispheric, seasonal and latitudinal dependence of storm-time ionosphere during low solar activity period, *Adv. Space Res.* **54**, 11, 2184-2193, DOI: 10.1016/j.asr.2014.08.013.

Adekoya, B.J., V.U. Chukwuma, N.O. Bakare, and T.W. David (2012a), On the effects of geomagnetic storms and pre storm phenomena on low and middle latitude ionospheric F2, *Astrophys. Space Sci.* **340**, 2, 217-235, DOI: 10.1007/s10509-012-1082-x.

Adekoya, B.J., V.U. Chukwuma, N.O. Bakare, and T.W. David (2012b), Effects of geomagnetic storm on middle latitude ionospheric F2 during storm of 2-6 April 2004, *Indian J. Rad. Space Phys.* **41**, 6, 606-616.

Adekoya, B.J., V.U. Chukwuma, and S.A. Salako (2013), On the coexistence of positive and negative ionospheric storm during geomagnetic storms and pre storm phenomena on low and low-mid latitude ionospheric F2. **In:** *Proc. 5th Nat. Ann. Conf. Nigerian Union of Radio Science (NURS)*, 15-28.

Adeniyi, J.O. (1986), Magnetic storm effects on the morphology of the equatorial F2-layer, *J. Atmos. Sol.-Terr. Phys*. **48**, 8, 695-702, DOI: 10.1016/0021-9169(86)90019-X.

Akala, A.O., E.O. Oyeyemi, E.O. Somoye, A.B. Adeloye, and A.O. Adewale (2010), Variability of foF2 in the African equatorial ionosphere, *Adv. Space Res*. **45**, 11, 1311-1314, DOI: 10.1016/j.asr.2010.01.003.

Bakare, N.O., and V.U. Chukwuma (2010), Relationship between Dst and solar wind conditions during intense geomagnetic storms, *Indian J. Rad. Space Phys.* **39**, 3, 150-155.

Balan, N., K. Shiokawa, Y. Otsuka, T. Kikuchi, D. Vijaya Lekshmi, S. Kawamura, M. Yamamoto, and G.J. Bailey (2010), A physical mechanism of positive ionospheric storms at low latitudes and mid latitudes, *J. Geophys. Res*. **115**, A2, A02304, DOI: 10.1029/2009JA014515.

Balasis, G., I.A. Daglis, P. Kapiris, M. Mandea, D. Vassiliadis, and K. Eftaxias (2006), From pre-storm activity to magnetic storms: a transition described in terms of fractal dynamics, *Ann. Geophys*. **24**, 3557-3567, DOI: 10.5194/angeo-24-3557-2006.

Blagoveshchensky, D.V., and A.S. Kalishin (2009), Increase in the critical frequency of the ionospheric F region prior to the substorm expansion phase, *Geomagn. Aeron*. **49**, 2, 200-209, DOI: 10.1134/S0016793209020091.

Buonsanto, M.J. (1999), Ionospheric storms – A review, *Space Sci. Rev.* **88**, 3-4, 563-601, DOI: 10.1023/A:1005107532631.

Burešová, D., and J. Laštovička (2007), Pre-storm enhancements of foF2 above Europe, *Adv. Space Res*. **39**, 8, 1298-1303, DOI: 10.1016/j.asr.2007.03.003.

Burešová, D., and J. Laštovička (2008), Pre-storm electron density enhancements at middle latitudes, *J. Atmos. Sol.-Terr. Phys.* **70**, 15, 1848-1855, DOI: 10.1016/j.jastp.2008.01.014.

Choe, G.S., N. LaBelle-Hamer, B.T. Tsurutani, and L.C. Lee (1992), Identification of a driver gas boundary layer, *EOS Trans. AGU* **73**, 485.

Chukwuma, V.U. (2007), On positive and negative ionospheric storms, *Acta Geod. Geoph. Hung*. **42**, 1, 1-21, DOI: 10.1556/AGeod.42.2007.1.1.

Dal-Lago, A., L.E.A. Vieira, E. Echer, W.D. Gonzalez, A.L. Clúa de Gonzalez, F.L. Guarnieri, L. Balmaceda, J. Santos, M.R. da Silva, A. de Lucas, and N.J. Schuch (2004), Great geomagnetic storms in the rise and maximum of solar cycle 23, *Braz. J. Phys*. **34**, 4B, 1542-1546, DOI: 10.1590/S0103-97332004000800008.

Danilov, A.D. (2001), F2-region response to geomagnetic disturbances, *J. Atmos. Sol.-Terr. Phys*. **63**, 5, 441-449, DOI: 10.1016/s1364-6826(00)00175-9.

Danilov, A.D. (2013), Ionospheric F-region response to geomagnetic disturbances, *Adv. Space Res.* **52**, 3, 343-366, DOI: 10.1016/j.asr.2013.04.019.

Davis, C.J., M.N. Wild, M. Lockwood, and Y.K. Tulunay (1997), Ionospheric and geomagnetic responses to changes in IMF Bz: a superposed epoch study, *Ann. Geophys*. **15**, 2, 217-230, DOI: 10.1007/s00585-997-0217-9.

Echer, E., M.V. Alves, and W.D. Gonzalez (2005), A statistical study of magnetic cloud parameters and geoeffectiveness, *J. Atmos. Sol.-Terr. Phys*. **67**, 10, 839-852, DOI: 10.1016/j.jastp.2005.02.010.

Fejer, B.G. (1997), The electrodynamics of the low-latitude ionosphere: Recent results and future challenges, *J. Atmos. Sol.-Terr. Phys*. **59**, 13, 1465-1482, DOI: 10.1016/S1364-6826(96)00149-6.

Foster, J.C., and F.J. Rich (1998), Prompt midlatitude electric field effects during severe geomagnetic storms, *J. Geophys. Res*. **103**, A11, 26367-26372, DOI: 10.1029/97JA03057.

Gonzalez, W.D., and B.T. Tsurutani (1987), Criteria of interplanetary parameters causing intense magnetic storms ($D_{st} < -100$ nT), *Planet. Space Sci*. **35**, 9, 1101-1109, DOI: 10.1016/0032-0633(87)90015-8.

Gonzalez, W.D., J.A. Joselyn, Y. Kamide, H.W. Kroehl, G. Rostoker, B.T. Tsurutani, and V.M. Vasyliunas (1994), What is a geomagnetic storm?, *J. Geophys. Res.* **99**, A4, 5771-5792, DOI: 10.1029/93JA02867.

Gonzalez, W.D., B.T. Tsurutani, and A.L. Clúa de Gonzalez (1999), Interplanetary origin of geomagnetic storms, *Space Sci. Rev*. **88**, 3-4, 529-562, DOI: 10.1023/A:1005160129098.

Gonzalez, W.D., B.T. Tsurutani, R.P. Lepping, and R. Schwenn (2002), Interplanetary phenomena associated with very intense geomagnetic storms, *J. Atmos. Sol.-Terr. Phys*. **64**, 2, 173-181, DOI: 10.1016/S1364-6826(01)00082-7.

Gonzalez, W.D., E. Echer, A.L. Clua-Gonzalez, and B.T. Tsurutani (2007), Interplanetary origin of intense geomagnetic storms (Dst < –100 nT) during solar cycle 23, *Geophys. Res. Lett*. **34**, 6, L06101, DOI: 10.1029/2006 GL028879.

Kamide, Y., N. Yokoyama, W. Gonzalez, B.T. Tsurutani, I.A. Daglis, A. Brekke, and S. Masuda (1998), Two-step development of geomagnetic storms, *J. Geophys. Res.* **103**, A4, 6917-6921, DOI: 10.1029/97JA03337.

Kane, R.P. (1975), Global evolution of the ionospheric electron content during some geomagnetic storms, *J. Atmos.-Terr. Phys.* **37**, 4, 601-611, DOI: 10.1016/ 0021-9169(75)90055-0.

Kane, R.P. (2005), Ionospheric foF2 anomalies during some intense geomagnetic storms, *Ann. Geophys*. **23**, 2487-2499, DOI: 10.5194/angeo-23-2487-2005.

Liu, J., B. Zhao, and L. Liu (2010), Time delay and duration of ionospheric total electron content responses to geomagnetic disturbances, *Ann. Geophys*. **28**, 3, 795-805, DOI: 10.5194/angeo-28-795-2010.

Liu, L., W. Wan, M.-L. Zhang, and B. Zhao (2008), Case study on total electron content enhancements at low latitudes during low geomagnetic activities before the storms, *Ann. Geophys*. **26**, 4, 893-903, DOI: 10.5194/angeo-26-893-2008.

Mikhailov, A.V., and L. Perrone (2009), Pre-storm NmF2 enhancements at middle latitudes: delusion or reality? *Ann. Geophys*. **27**, 3, 1321-1330, DOI: 10.5194/angeo-27-1321-2009.

Mikhailov, A.V., M.G. Skoblin, and M. Förster (1995), Daytime F2-layer positive storm effect at middle and lower latitudes, *Ann. Geophys*. **13**, 5, 532-540, DOI: 10.1007/s00585-995-0532-y.

Prölss, G.W. (1993), On explaining the local time variation of ionospheric storm effects, *Ann. Geophys*. **11**, 1, 1-9.

Prölss, G.W. (1995), Ionospheric F-region storms. **In:** H. Volland (ed.), *Handbook of Atmospheric Electrodynamics*, Vol. 2, CRC Press, Boca Raton, 195-248.

Saranya, P.L., K. Venkatesh, D.S.V.V.D. Prasad, P.V.S. Rama Rao, and K. Niranjan (2011), Pre-storm behaviour of NmF_2 and TEC (GPS) over equatorial and low latitude stations in the Indian sector, *Adv. Space Res*. **48**, 2, 207-217, DOI: 10.1016/j.asr.2011.03.028.

Sutton, E.K., J.M. Forbes, R.S. Nerem, and T.N. Woods (2006), Neutral density response to the solar flares of October and November 2003, *Geophys. Res. Lett.* **33**, 22, L22101, DOI: 10.1029/2006GL027737.

Vieira, L.E.A., W.D. Gonzalez, A.L. Clua de Gonzalez, and A. Dal Lago (2001), A study of magnetic storms development in two or more steps and its association with the polarity of magnetic clouds, *J. Atmos. Sol.-Terr. Phys*. **63**, 5, 457-461, DOI: 10.1016/S1364-6826(00)00165-6.

Vijaya Lekshmi, D., N. Balan, S. Tulasi Ram, and J.Y. Liu (2011), Statistics of geomagnetic storms and ionospheric storms at low and mid latitudes in two solar cycles, *J. Geophys. Res*. **116**, A11, A11328, DOI: 10.1029/2011JA017042.

Wang, C.B., J. K. Chao, and C.H. Lin (2003), Influence of the solar wind dynamic pressure on the decay and injection of the ring current, *J. Geophys. Res*. **108**, A9, 1341, DOI: 10.1029/2003JA009851.

Received 17 April 2014
Received in revised form 4 September 2014
Accepted 26 November 2014